Requirements of Slm proteins for proper eisosome organization, endocytic trafficking and recycling in the yeast *Saccharomyces cerevisiae*

CHITRA KAMBLE†, SANDHYA JAIN†, ERIN MURPHY and KYOUNGTAE KIM*

Department of Biology, Missouri State University, 901 South National Ave, Springfield, MO 65897, USA

†*These authors contributed equally to this work.*

**Corresponding author (Fax, +417-836-5126; Email, kkim@missouristate.edu)*

Eisosomes are large immobile assemblies at the cortex of a cell under the membrane compartment of Can1 (MCC) in yeast. Slm1 has recently been identified as an MCC component that acts downstream of Mss4 in a pathway that regulates actin cytoskeleton organization in response to stress. In this study, we showed that inactivation of Slm proteins disrupts proper localization of the primary eisosome marker Pil1, providing evidence that Slm proteins play a role in eisosome organization. Furthermore, we found that *slm*^{ts} mutant cells exhibit actin defects in both the ability to polarize cortical F-actin and the formation of cytoplasmic actin cables even at the permissive temperature (30°C). We further demonstrated that the actin defect accounts for the slow traffic of FM4-64-labelled endosome in the cytoplasm, supporting the notion that intact actin is essential for endosome trafficking. However, our real-time microscopic analysis of Abp1-RFP revealed that the actin defect in *slm*^{ts} cells was not accompanied by a noticeable defect in actin patch internalization during receptor-mediated endocytosis. In addition, we found that *slm*^{ts} cells displayed impaired membrane recycling and that recycling occurred in an actin-independent manner. Our data provide evidence for the requirement of Slm proteins in eisosome organization and endosome trafficking and recycling.

[Kamble C, Jain S, Murphy E and Kim K 2011 Requirements of Slm proteins for proper eisosome organization, endocytic trafficking and recycling in the yeast *Saccharomyces cerevisiae*. *J. Biosci.* **36** 79–96] **DOI** 10.1007/s12038-011-9018-0

1. Introduction

Endocytosis is a process by which extracellular materials and components of the plasma membrane are internalized and then either targeted to the lysosome for degradation or recycled back to the plasma membrane to support membrane homeostasis (Shaw *et al.* 2001; Liu *et al.* 2009). The hallmark events of early endocytosis include invagination of the plasma membrane, followed by the pinching off of the endocytic vesicle (Shaw *et al.* 2001; Drubin *et al.* 2005; Walther *et al.* 2006; Liu *et al.* 2009). Although the stepwise recruitment of endocytic components, as well as their membrane dynamics during the internalization of endocytic vesicles, is well documented, little is known about the molecular mechanism by which the endocytic site is selected on the plasma membrane. A previous study provided, for the first time, an important clue – eisosome, a large immobile protein complex on the plasma membrane, coincides with known endocytic markers (Walther *et al.* 2006). More recently, it has been found that a number of

Keywords. Actin; actin patch; eisosome; endocytosis; endosome; FM4-64; Pil1; recycling; Slm1/2; trafficking

Abbreviations used: FITC, fluorescein isothiocyanate; LCB, long-chain bases; LY, Lucifer yellow; MCC, membrane compartment of Can1; MCP, membrane compartment of Pma1; NA, numerical aperture; PH, pleckstrin homology; RME, receptor-mediated endocytosis; YPD, yeast peptone dextrose

eisosome components including Pil1, Lsp1 and Sur7 are associated with a patch-like membrane compartment called membrane compartment of Can1 (MCC) (Grossmann *et al.* 2008). However, they showed that the eisosome marker Sur7 does not colocalize with sites of classical endocytosis, seemingly contradictory to the observation made by Walther *et al.* (2006). Among many eisosome components, on the basis of the observation that *PIL1*-deficient cells displayed a severe disruption of the eisosome, Pil1 appears to play a central role in organizing the eisosome (Walther *et al.* 2006; Grossmann *et al.* 2007). Subsequently, it was found that eisosomes disassemble when Pil1 is hyperphosphorylated by the overexpressed Pkh-kinases and by the reduction of sphingolipid long-chain bases (LCB) levels, whereas the eisosome assembly is enhanced when Pil1 is hypophosphorylated (Walther *et al.* 2007). Nce102, a multispanning plasma membrane protein, is another component necessary for the structural integrity of the eisosome because the eisosome marker Sur7 disperses laterally throughout the plasma membrane upon loss of Nce102 (Grossmann *et al.* 2008). Similarly, the targeting of Pil1 to the eisosome is affected by the loss of Nce102 (Frohlich *et al.* 2009). The current view of the mechanism of action of Nce102 is that it negatively regulates Pil1 phosphorylation by inhibiting Pkh-kinases (Frohlich *et al.* 2009). At least 88 genes appear to be involved in eisosome organization, according to a genome-wide screen for genes that affect Pil1-GFP localization, which include genes participating in endocytosis (*ENT4* and *RCY1*) and in endosome trafficking (*PEP8, VPS51* and *VPS53*) (Frohlich *et al.* 2009).

The long list of eisosome components includes the Slm proteins (Slm1/2) because Slm1 colocalizes with Sur7, an eisosome marker (Grossmann *et al.* 2008). Previous studies have shown that Slm1 and its homologue Slm2 bind to phosphatidylinositol 4,5-biphosphate (PIP_2) enriched at the plasma membrane via their pleckstrin homology (PH) domain (Audhya *et al.* 2004; Yu *et al.* 2004; Fadri *et al.* 2005). The membrane targeting of the Slm proteins was affected in *mss4* mutant cells that expressed a fraction of the normal amount of PIP_2, suggesting that the membrane recruitment of Slm1/2 depends on an optimal endogenous level of PIP_2 (Desrivieres *et al.* 1998; Homma *et al.* 1998; Yu *et al.* 2004). It seems that the membrane targeting of Slm proteins are further assisted in part by their interaction with the Avo2 and Bit61 subunits of TORC2, which mediates Tor2 signalling to the actin cytoskeleton (Schmidt *et al.* 1996; Audhya *et al.* 2004; Fadri *et al.* 2005; Dickson 2008). Therefore, an increasing body of evidence supports the idea that Slm1/2 function downstream of both the PIP_2-producing Mss4 and TORC2 signalling pathways, as inactivation of *SLM1* in the background of *slm2Δ* at the non-permissive temperature mimics the phenotype of *mss4* and *tor2* mutant cells manifested by severe actin defects (Audhya and Emr 2002, 2003; Fadri *et al.* 2005).

In addition, Slm proteins seem to be involved in polarized growth in yeast. It is known that actin cables are required for the proper targeting of two Rho GTPases, Cdc42 and Rho1, to the sites of polarized growth, such as the growing bud (Abe *et al.* 2003; Wedlich-Soldner *et al.* 2003; Pruyne *et al.* 2004; Fadri *et al.* 2005). Interestingly, actin cables were severely disrupted in slm^{ts} mutant cells, and as a result, Rho1 and Cdc42 are dispersed throughout the cytoplasm rather than being concentrated at the site of polarized growth (Fadri *et al.* 2005). This result indicates a functional connection between the Slm proteins and the two downstream effectors, Cdc42 and Rho1, in regulating polarized growth in yeast by maintaining the structural integrity of actin cables (Fadri *et al.* 2005). Finally, Slm proteins are implicated in heat-stress-induced endocytosis of the uracil permease, Fur4, which undergoes ubiquitination prior to its internalization (Galan *et al.* 1996; Blondel *et al.* 2004; Bultynck *et al.* 2006). This was based on the observation that ubiquitinated Fur4 accumulated at the surface of *slm1* temperature-sensitive mutant cells.

The recent findings of Slm proteins being colocalized with the eisosome marker Sur7 (Grossmann *et al.* 2008) and the participation of Slm proteins in endocytosis of Fur4 (Bultynck *et al.* 2006) raise new questions about the physiological significance of Slm1/2 in eisosome organization and the details of how they function in endocytosis. In this study we demonstrated that Slm1 colocalizes with the eisosome marker Pil1 and that Slm proteins are required for the structural integrity of the eisosome. Using live cell imaging, we showed that Slm mutations affect the transit of FM4-64 both at permissive (30°C) and non-permissive (37°C) temperatures and that the reason underlying the comparatively slow rate of endocytosis is due to the perturbed intracellular endosome motility, caused mainly by actin disruption in those conditions. In addition, we reveal that Slm proteins function in membrane recycling in an actin-independent manner.

2. Materials and methods

2.1 *Yeast strain construction and media*

The yeast strains used in this study are listed in table 1. Yeast strains expressing Pil1-RFP, Pma1-RFP, Abp1-RFP or Slm1-GFP were constructed by integrating the respective RFP or GFP constructs at the 3′ end of the *PIL1*-, *PMA1*-, *ABP1*- or *SLM1*-coding regions as described previously (Longtine *et al.* 1998; Kim *et al.* 2006; Nannapaneni *et al.* 2010) in a wild-type haploid (BY 4741 or 4742). Similarly, Slm1-GFP in *pil1Δ*, Pil1-GFP in *slm1Δ*, Pil1-RFP in *slm1Δ*, and Pil1-RFP or Abp1-RFP in *slm1-2slm2Δ* and *slm1-3slm2Δ* were constructed by integrating the respective RFP or GFP constructs in each mutant strain. Three slm^{ts} mutants (*slm1-2slm2Δ, slm1-3slm2Δ* and *slm1-5slm2Δ*) were obtained from Dr Scott Emr's laboratory. All yeast strains were grown in standard yeast peptone dextrose (YPD) medium with appropriate amino acids and were cultured at 30°C, unless otherwise stated.

Table 1. Yeast strains used in this study

Strain	Source	Genotype
KKY 0038	Evangelista *et al.* 2002	*Mat α BNR1::KanR his3Δ leu2Δ lys2Δ ura3Δ*
KKY 0040	Evangelista *et al.* 2002	*Mat α BNR1::KanR bni1-12::URA3 his3Δ leu2Δ lys2Δ ura3Δ*
KKY 0082	Invitrogen	*Mat a his3Δ leu2Δ met15Δ ura3Δ RCY1::KanMX6*
KKY 0193	Invitrogen	*Mat α his3Δ leu2Δ lys2Δ ura3Δ SLM1::KanMX6*
KKY 0197	Invitrogen	*Mat α his3Δ leu2Δ lys2Δ ura3Δ*
KKY 0233	This study	*Mat a SLM1-GFP-HIS his3Δ1 leu2Δ ura3Δ met15Δ PIL1::KanMX6*
KKY 0236	This study	*Mat a PIL1-GFP-HIS his3Δ1 leu2Δ ura3Δ met15Δ SLM1::KanMX6*
KKY 0289	This study	*Mat a Pil1-KanMX6-RFP, SLM1-GFP-HIS his3Δ1 leu2Δ met15Δ ura3Δ*
KKY 0299	This study	*Mat a his3Δ leu2Δ met15Δ ura3Δ SLM2::HIS*
KKY 0323	Audhya *et al.* 2004	*Mat α leu2-3,112 ura3-53 his3-Δ200 trp1-Δ901 lys2-801 suc2-Δ9 Slm1Δ::HIS3 Slm2Δ::HIS3 carrying pRS415 slm1-2 (LEU2 CEN6 slm1-2)*
KKY 0324	Audhya *et al.* 2004	*Mat α leu2-3,112 ura3-53 his3-Δ200 trp1-Δ901 lys2-801 suc2-Δ9 Slm1Δ::HIS3 Slm2Δ::HIS3 carrying pRS415 slm1-3 (LEU2 CEN6 slm1-3)*
KKY 0326	Audhya *et al.* 2004	*Mat α leu2-3,112 ura3-53 his3-Δ200 trp1-Δ901 lys2-801 suc2-Δ9 Slm1Δ::HIS3 Slm2Δ::HIS3 carrying pRS415 slm1-5 (LEU2 CEN6 slm1-5)*
KKY 0336	This study	*Mat α leu2-3,112 ura3-53 his3-Δ200 trp1-Δ901 lys2-801 suc2-Δ9 Slm1Δ::HIS3 Slm2Δ::HIS3 carrying pRS415 slm1-5 (LEU2 CEN6 slm1-5), ABP1-RFP-KanMX*
KKY 0337	This study	*Mat α leu2-3,112 ura3-53 his3-Δ200 trp1-Δ901 lys2-801 suc2-Δ9 Slm1Δ::HIS3 Slm2Δ::HIS3 carrying pRS415 slm1-2 (LEU2 CEN6 slm1-2), PIL1-RFP-KanMX6*
KKY 0340	This study	*Mat α leu2-3,112 ura3-53 his3-Δ200 trp1-Δ901 lys2-801 suc2-Δ9 Slm1Δ::HIS3 Slm2Δ::HIS3 carrying pRS415 slm1-2 (LEU2 CEN6 slm1-2), ABP1-RFP-KanMX6*
KKY 0341	This study	*Mat α leu2-3,112 ura3-53 his3-Δ200 trp1-Δ901 lys2-801 suc2-Δ9 Slm1Δ::HIS3 Slm2Δ::HIS3 carrying pRS415 slm1-3 (LEU2 CEN6 Slm1-3), ABP1-RFP-KanMX*
KKY 0491	This study	*Mat a ura3Δ trp1Δ leu2Δ his3Δ ade2Δ can1-100 TLG1::HIS*
KKY 0492	This study	*Mat a ura3Δ trp1Δ leu2Δ his3Δ ade2Δ can1-100 TLG2::HIS*
KKY 0357	This study	*Mat α his3Δ leu2Δ lys2Δ ura3Δ SLM1::KanMX6*
KKY 0403	This study	*Mat α leu2-3,112 ura3-53 his3-Δ200 trp1-Δ901 lys2-801 suc2-Δ9 Slm1Δ::HIS3 Slm2Δ::HIS3 carrying pRS415 slm1-3 (LEU2 CEN6 slm1-3), PIL1-RFP-KanMX6*
KKY 0434	This study	*Mat α leu2-3,112 ura3-52 his3-Δ200 trp1-Δ901 lys2-801 suc2-Δ9 SLM1-GFP-HIS*
KKY 0441	This study	*Mat a his3Δ1 leu2Δ met15Δ ura3Δ SLM1-GFP-HISMx6, PMA1-RFP-KanMX6*
KKY 0473	This study	*Mat a his3Δ leu2Δ lys2Δ ura3Δ, ABP1-RFP-KanMX6*
KKY 0604	This study	*Mat α his3Δ leu2Δ lys2Δ ura3Δ PIL1-RFP-KanMX6*
KKY 0620	This study	*Mat α his3Δ leu2Δ lys2Δ ura3Δ, ABP1-RFP-KanMX6, SLM1-GFP-HIS*
KKY 0641	This study	*Mat α his3Δ leu2Δ lys2Δ ura3Δ, SLM2::HIS, ABP1-RFP-KanMX6*
KKY 0648	This study	*Mat a His 3Δ leu2 Δ met15Δ ura3Δ SLM2::HIS,STE2-CFP-KanMX6*
KKY 0655	This study	*Mat α his3Δ leu2Δ lys2Δ ura3Δ STE2-CFP-KanMX6*
KKY 0667	This study	*Mat α leu2-3,112 ura3-53 his3-Δ200 trp1-Δ901 lys2-801 suc2-Δ9 Slm1Δ::HIS3 Slm2Δ::HIS3 carrying pRS415 slm1-3 (LEU2 CEN6 slm1-3) STE2-CFP-KanMx6*
KKY 0691	This study	*Mat a PIL1-RFP-KanMX6 his3Δ1 leu2Δ ura3Δ met15Δ SLM1::HIS*

2.2 *Light microscopy*

Time-lapse movies of GFP-, RFP- or FM4-64-labelled cells were made with a spinning disk confocal system that included an upright Olympus IX81 microscope, a Yokogawa CSUX1 spinning disk head, a 100× numerical aperture (NA) 1.4 PlanApo oil objective and an Electron Amplified CCD (ImagEM, Hamamatsu). The temperature of the specimen and stage was maintained at 30°C, except in temperature shift experiments. For temperature shift experiments, cells were gown overnight at 30°C to an optical density of ~0.3 at 600 nm and were placed in a shaker incubator for 90 min at 37°C prior to imaging. The image was focused at an equatorial plane of the cells. Movies were recorded with a frame rate of 3 images per second for 60 s.

2.3 *FM4-64 pulse-chase labelling*

Cells were incubated with FM4-64 dye as described previously (Kim *et al.* 2006; Nannapaneni *et al.* 2010) but with a few modifications. Briefly, cells were grown in YPD media overnight, incubated with 12 µl of FM4-64 (1 mM) on ice for 10 min, and washed with ice-cold SD-complete medium. The cells were resuspended in fresh ice-cold SD medium and kept at 30°C (or 37°C in temperature shift experiments) in an incubator for 30 min. FM4-64-labelled cells were examined using a conventional fluorescence microscope [Leica, DMI6000B inverted microscope equipped with a 100× oil NA 1.4 objective lens, a Rhodamine filter cube, and an Orca Digital camera (Hamamatsu) controlled by IPLab software]. On the basis of the subcellular distribution of FM4-64, cells were grouped into the following phases. phase I: FM4-64 foci found exclusively on the plasma membrane with very few in the cytoplasm; phase II: FM4-64 foci found primarily in the cytoplasm with very few on the plasma membrane; phase III: FM4-64 found at the rim of the vacuole. Nearly 100 cells were utilized for each experiment, and the experiment was repeated three times to determine the mean value and standard deviation.

2.4 *Actin staining with fluorescein isothiocyanate-Phalloidin*

Cells were stained with fluorescein isothiocyanate (FITC)-Phalloidin as previously described (Sizonenko *et al.* 1996; Kim *et al.* 2004). The cells were grown overnight in YPD medium and fixed in 1× PBS containing formaldehyde (10% final concentration). The fixed cells were then permeabilized with 0.1% Triton-X-100, followed by brief sonication for 10–12 s and staining with FITC-Phalloidin (3 µM final concentration) for 15 min. Fluorescence images of actin at either 30°C or 37°C were made with the spinning disk confocal system, as stated earlier, with an exposure time of 100 ms. The extent of the actin cytoskeleton polarization was determined as described before (Kim *et al.* 2004); cells that carry less than five actin patches in the mother portion of small-budded cells are defined as polarized cells. Quantification of the cytoplasmic actin cable was carried out on the basis of the actin cable structure. Cells containing actin cables running parallel to the longitudinal axis of the cell were grouped into 'intact cable cells'.

2.5 *Measurement of patch lifetime at the membrane and kymograph*

The lifetime an Abp1-RFP patch at the membrane (from the time of its appearance to the time at which it moves away from its origin or disappears) was determined as described previously (Nannapaneni *et al.* 2010). A total of 20–25 patches were measured to determine the average patch lifespan of a strain. Patches that at any point in their lifetimes were too close to another patch to be clearly resolved were excluded from our analysis. A kymographic representation of Abp1-RFP in a single patch over time was made using SlideBook (v.5).

2.6 *Computer-assisted tracking of patch movement*

The motile behaviour of Abp1-RFP patches was assessed as mentioned previously (Carlsson *et al.* 2002; Kim *et al.* 2006; Nannapaneni *et al.* 2010). Briefly, the character and degree of patch motion was analysed by calculating the square of the patch distance (μm^2) from the origin over time. The distance value obtained from at least 20–25 patches was averaged to determine the mean squared displacement (MSD, μm^2) and plotted as a function of time. Similarly, the motile behaviour of FM4-64-labelled endosome was assessed. Cells were incubated with 12 µM of FM4-64 for 5 min at 30°C, washed three times to remove the excess dye and kept on ice. The cells were then incubated for 3–4 min prior to a time-lapse live-cell imaging of FM4-64-labelled endosome with a frame rate of 4 images per second for 40 s with the spinning confocal system. At least 10 mobile endosomes selected randomly from each strain was manually traced using SlideBook (v.5), and the MSD was plotted as a function of time.

2.7 *FM4-64 recycling assay*

Cells were allowed to internalize FM4-64 for 12 min as described earlier and the recycling assays were performed as described previously (Wiederkehr *et al.* 2000), with a few modifications. Briefly, cells were incubated with 40 µM of FM4-64 at room temperature for 10 min and washed three times with ice-cold SD-complete medium. After the last wash step, the cells were resuspended in 10 µl ice-cold SD-complete

medium and kept on ice. Pre-warmed (room temperature) SD medium was added to the cells to a final optical density A_{600} of 0.25. The cell suspension (3 ml) was added to a cuvette. FM4-64 fluorescence was recorded at an angle of 90° on a Perkin Elmer Spectrofluorometer. Excitation was at 515 nm with a bandwidth of 10 nm, and emission was measured at 680 nm with a bandwidth of 10 nm.

3. Results

3.1 *Spatial relationship between Slm1 with Pil1 and endocytic markers*

Previously, a group of researchers (Grossmann *et al.* 2008) identified Slm1 as a component of membrane compartment of Can1 (MCC). Many MCC markers, including Sur7, have been found to be colocalized to the eisosome marker (Pil1) that plays a pivotal role in the organization of the eisosome (Walther *et al.* 2006; Grossmann *et al.* 2008). We thus envisioned that Slm1 might colocalize with Pil1 and examined the spatial relationship between them. To study this, a wild-type (WT) strain coexpressing Slm1-GFP and Pil1-RFP was constructed and subjected to spinning cofocal microscopic analysis. As shown in figure 1A, not all but a majority of Slm1-GFP patches were found to colocalize with Pil1-RFP. Approximately 70% of Pil1-RFP cortical patches were colocalized with Slm1-GFP, and 60% of Slm1-GFP patches were colocalized with Pil1-RFP. In a previous study, Slm1 was found to colocalize with the membrane compartment of Pma1 (MCP) marker Pma1 (Fadri *et al.* 2005). However, Pma1 was not coincided with the eisosome protein Sur7 in another localization study (Malinska *et al.* 2004). To resolve these seemingly contradictory results, we examined the spatial relationship between Slm1-GFP and Pma1-RFP. Pma1-RFP fluorescence displayed a fairly uniform staining of the plasma membrane (figure 1B, middle panel), whereas Slm1-GFP showed a characteristic punctuate pattern of MCC. Slm1-GFP appeared to partially colocalize with Pma1-RFP (figure 1B, top and middle panels) because of the uniform distribution of Pma1-RFP. As indicated (figure 1C, D), a minor fraction of Slm1-GFP at the cell cortex spatially overlapped with Abp1-RFP and FM4-64 carrying endocytic patches.

3.2 *Disruption of eisosome organization in slm^{ts} mutants*

Studies have shown that loss of Pil1 resulted in a severe disruption of eisosome markers, including Can1, Sur7 and Lsp1 (Walther *et al.* 2006; Grossmann *et al.* 2008). Having confirmed that Slm1 colocalizes with Pil1, we further investigated whether the loss of Pil1 affects the localization of Slm1-GFP. A few large aggregates carrying Slm1-GFP were seen near the membrane in *PIL1*-deficient cells (figure 2A, left-hand panel), consistent with the idea that Pil1 is required for stable eisosome formation. In contrast, Pil1 was properly targeted to the membrane cortex in *slm1Δ* cells (figure 2A, right-hand panel). To investigate the possibility of Slm2 functionally compensating for the loss of Slm1, we analysed Pil1 localization in two *slm^{ts}* mutants (*slm1-2slm2Δ* and *slm1-3slm2Δ*) expressing Pil1-RFP. In temperature shift experiments, the cells were first cultured overnight at 30°C, and the temperature was then shifted to 38°C for 90 min to inactivate mutant Slm1 proteins. As expected, in WT and *slm1Δ* cells at both temperature sets, we found that Pil1-RFP-carrying eisosomes were evenly distributed at the membrane cortex (figure 2B, first and second rows). However, inactivation of Slm1 in the *slm2Δ* background at the non-permissive but not the permissive temperature resulted in severe defects in Pil1 localization. First, fewer and weaker Pil1-RFP foci were found at the cell cortex, and second, the cytoplasmic dispersion of Pil1-RFP seemingly increased (figure 2B, third and fourth rows). Interestingly, the Pil1 localization in *slm^{ts}* mutants was restored when the temperature was shifted from 38°C to 30°C (data not shown). Thus, we have come to the conclusion that Slm1 and Slm2 are functionally redundant in eisosome organization and that either Slm1 or Slm2 is necessary and sufficient for the proper localization of Pil1 upon the loss of a homologue of the redundant pair.

3.3 *Slow FM4-64 transit in slm^{ts} mutants*

Fur4 is a uracil permease that mediates the uptake of uracil (Chevallier 1982; Kurtz *et al.* 1999) and is localized to the MCC compartment that contains Can1 and Sur7 (Malinska *et al.* 2004). Recently, Bultynck *et al.* (2006) showed that ubiquitinated Fur4 accumulated at the cell cortex of *slm^{ts}* cells, suggesting that Slm proteins are required for internalization of Fur4 at MCC. This finding raises the question of whether Slm proteins function in two known routes of endocytosis in yeast – pinocytosis and receptor-mediated endocytosis (RME). First, to test the possibility of Slm proteins contributing to uptake and the follow-up delivery of membrane lipid components via pinocytosis, the fluorescent lipophilic dye FM4-64 was pulse-chased at both the permissive (30°C) and the non-permissive (37°C) temperatures, as described previously (Nannapaneni *et al.* 2010). According to a previous kinetic analysis of FM4-64 (Vida and Emr 1995), delivery of the dye followed an endocytic transport route, from the plasma membrane, passing through intracellular endosome compartments, to the vacuole. In order to characterize any defects in endocytic transport of FM4-64, we divided the whole liquid-phase endocytosis into three phases on the basis of the subcellular distribution of the dye (*see* Methods). We first conducted the FM4-64 pulse-chase assay at the non-permissive temperature (37°C)

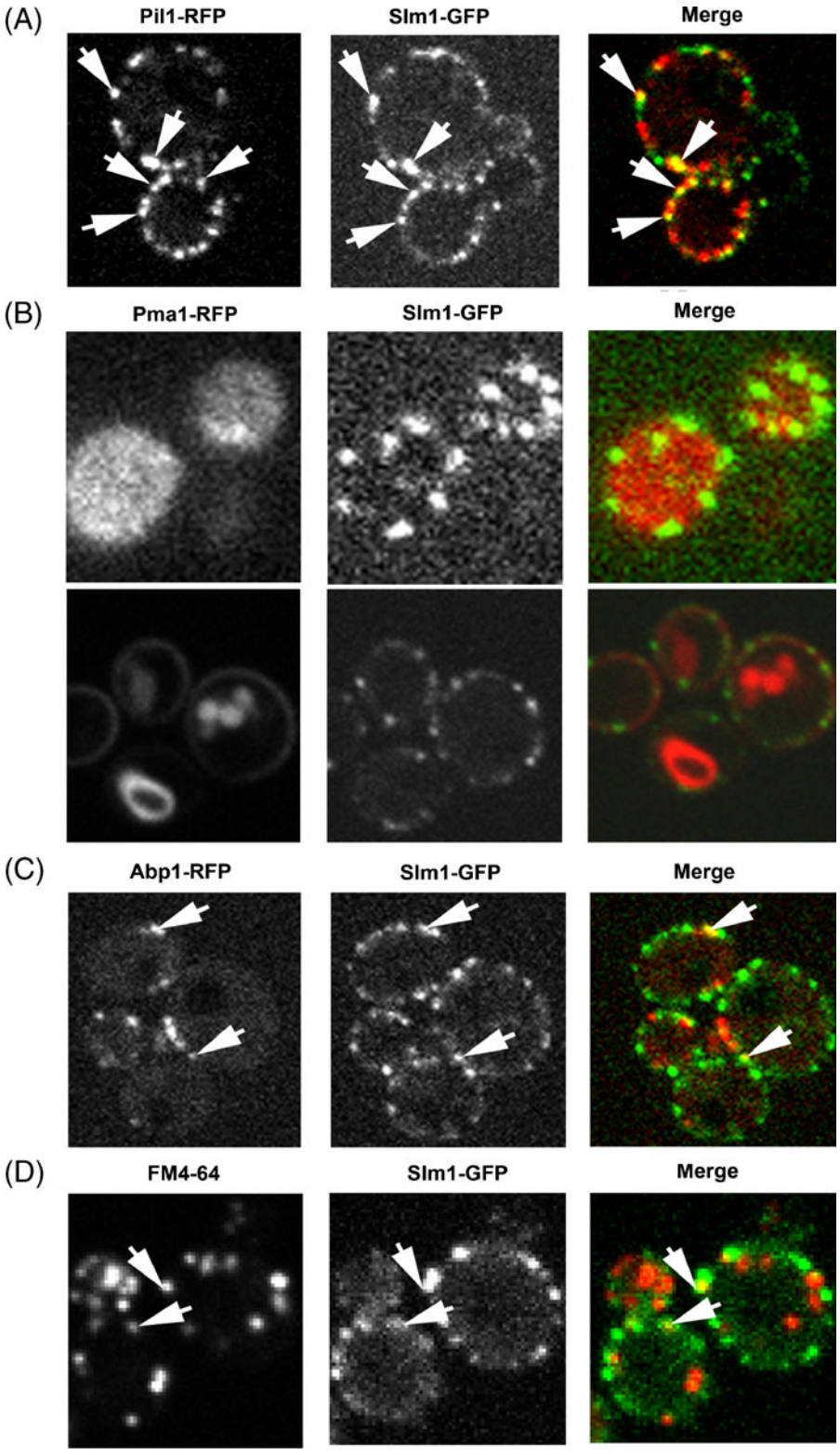

Figure 1. For caption, *see* page no. 85.

because of a severe defect in Fur4 uptake in cells lacking Slm protein activity at an elevated temperature (Bultynck *et al.* 2006). After the 30 min chase, WT cells were in phase III (figure 3A, B), with a clear sign of fusion of FM4-64 to the rim of the vacuole (arrow). Similarly, the majority of cells deficient in either Slm1 or Slm2 were found in phase III (figure 3A, B; vacuoles indicated by arrows). Only a small fraction (3%) of *slm2*Δ cells exhibited the accumulation of FM4-64 foci in the cytoplasm (phase II), whereas no *slm1*Δ cells were in phase II in the same condition (figure 3B). The lack of defects in the delivery of FM4-64 to the vacuole in single mutant cells (*slm1Δ* and *slm2Δ*) might be due to the possibility of a Slm homologue functionally compensating for the loss of the other. As expected, the FM4-64 transit to the vacuole was significantly impaired in all three *slm*^{ts} mutants (*slm1-2*, *slm1-3* and *slm1-5*) (figure 3A, B): First, FM4-64 accumulation in the cytoplasm increased significantly as compared with that in the WT (figure 3A). Second, most of the *slm1-2* cells were either in phase II (62.5%) or phase III (36.55%) as is the case for *slm1-3* (72% in phase II and 27.8% phase III) and *slm1-5* cells (70% in phase II and 29.2% phase III) (figure 3B). To our surprise, we found that all tested *slm*^{ts} cells at the permissive temperature (30°C) showed a significant defect in FM4-64 delivery to the vacuole (figure 3C), albeit less severe compared with that found at the non-permissive temperature. This suggests that the 'loss of function' Slm1 mutant species in *slm*^{ts} cells are not able to fully compensate for the loss of Slm2 even in the optimal temperature condition.

3.4 *Severe actin disruption at permissive temperature*

The observation of the FM4-64 transit defect in *slm*^{ts} cells even at the permissive temperature (30°C) prompted us to assess the effects of *SLM* gene inactivation on the actin cytoskeleton organization at this temperature. For this, WT and *slm* mutant cells (*slm1Δ*, *slm2Δ*, *slm1-2*, *slm1-3* and *slm1-5*) were stained with FITC-Phalloidin and subjected to fluorescence microscopic analysis. First, we determined the extent of actin polarization using at least 50 small-budded cells. As a quantitative measure, we counted the number of actin patches in the mother portion of small-budded cells and defined polarized cells as having <5 patches in the mother. At the permissive temperature (30°C), more than 90% of the WT cells showed actin patches concentrated in the bud, the site of polarized growth (figure 4A, B). The extent of actin patch polarization in *slm1Δ* (84%) and *slm2Δ* (84%) was nearly comparable to that of the WT cells (figure 4A, B). However, levels of actin patch polarization in *slm1-2*, *slm1-3* and *slm1-5* were significantly reduced by 24, 14 and 68%, respectively (figure 4A, B). Levels of actin patch polarization of WT (92%), *slm1Δ* (81%) and *slm2Δ* (86%) at the non-permissive temperature (37°C) were essentially identical (figure 4B) to those obtained in the above experiments done at 30°C. In contrast, patch polarization was severely disrupted in *slm*^{ts} cells with patch polarization levels of 5, 9 and 6% in *slm1-2*, *slm1-3* and *slm1-5* cells, respectively (figure 4B). Of note, the severe actin polarization defect found in *slm1-3* here is consistent with a previous study, which showed that approximately 90% of the mutant cells contained depolarized actin patches at 38°C (Fadri *et al.* 2005). In addition, we examined the cytoplasmic actin cable structure. Only cells with actin cables running parallel to the longitudinal axis of the cell were grouped into intact cable cells, and we excluded cells without the actin cable or with short fragmented cable (s). As shown in figure 4C, most of WT, *slm1Δ* and *slm2Δ* cells showed the intact cables at both 30°C and 37°C. However, the levels of intact actin cables at 30°C were significantly lower for *slm1-2* (22%), *slm1-3* (12%) and *slm1-5* (73%) than that for WT. None of the three temperature-sensitive mutants revealed intact cables at the non-permissive temperature (figure 4C). Thus, our sensitive actin assay revealed that the presence of either one of the two Slm homologues is sufficient for the structural integrity of the actin cytoskeleton and that a certain level of inactivation of Slm1 in *slm2Δ* background at even the permissive temperature (30°C) leads to actin defects in both actin patch polarization and the formation of intact actin cables.

3.5 *Slow endosome trafficking*

Previous studies have shown that the intact actin cable structure plays an important role in the trafficking of the endocytosed vesicles (hereafter, endosome) to late endo-

Figure 1. Colocalization study of Slm1 with eisosome component (Pil1) and endocytic markers (Abp1 and FM4-64). (**A**) Colocalization of Slm1 with Pil1. A WT strain coexpressing Slm1-GFP and Pil1-RFP (KKY 289) was used to examine the spatial relationship between Slm1 and Pil1. Note that the majority of Pil1-RFP cortical patches were colocalized to Slm1-GFP (shown by arrows). (**B**) No colocalization of Slm1 with Pma1. A WT strain coexpressing Slm1-GFP and Pma1-RFP (KKY 441) was used to examine the spatial relationship between Slm1 and Pma1. None of Slm1-GFP patches colocalized to Pma1-RFP. Note that the first and second rows in (**B**) indicate the top and middle views, respectively. (**C–D**) Partial colocalization of Slm1 with endocytic markers. (**C**) A WT strain coexpressing Slm1-GFP and Abp1-RFP (KKY 620) was used to examine colocalization between Slm1 and the receptor-mediated endocytosis marker Abp1. Interestingly, a few Slm1 patches colocalized with Abp1 (indicated by arrows). (**D**) A Slm1-GFP expressing WT strain (KKY 434) labelled with FM4-64, a lipophilic dye, was used to examine the colocalization between the liquid-phase endocytic marker FM4-64 and Slm1. Only a fraction of Slm1 patches colocalized with FM4-64, as indicated by arrows.

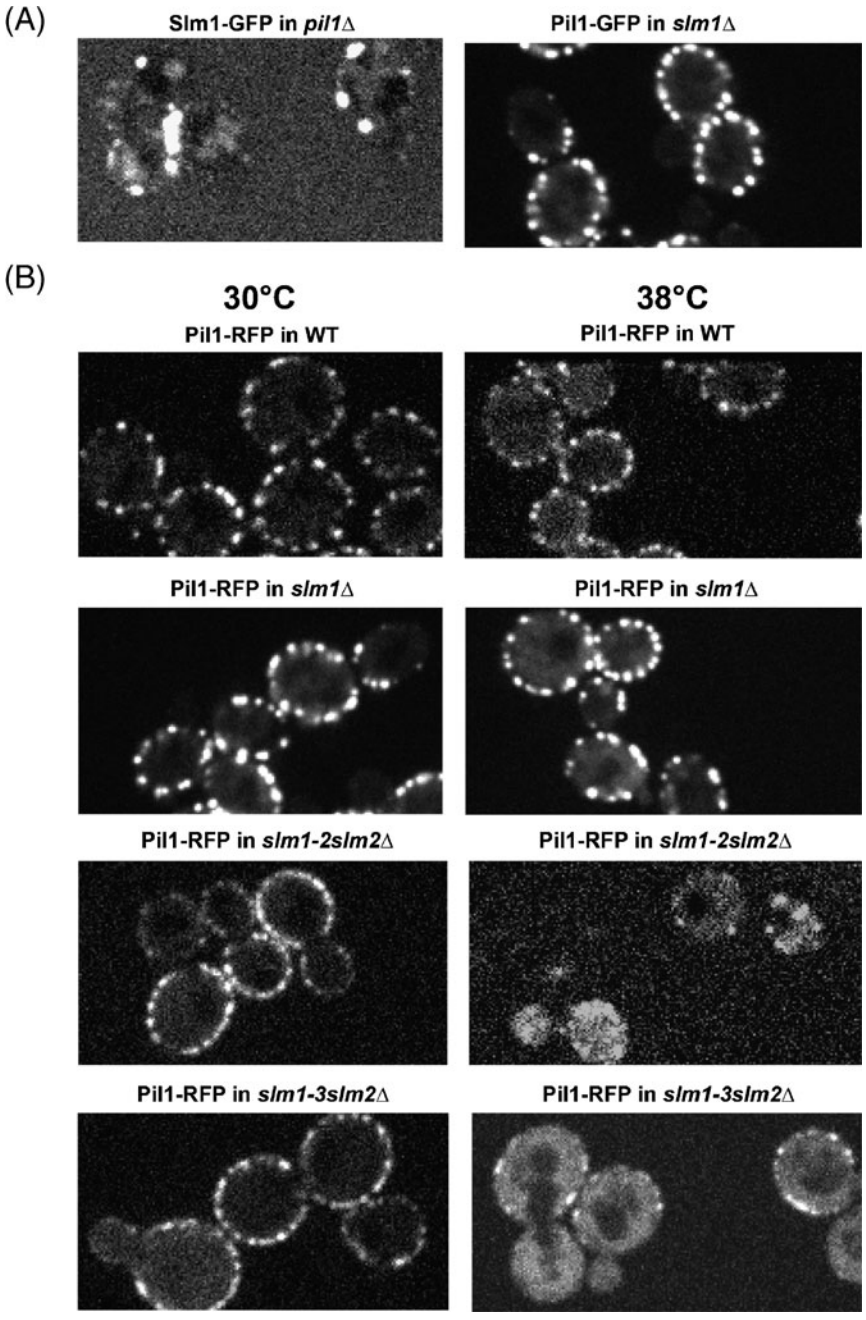

Figure 2. Inactivation of *SLM* genes affects eisosome organization. (**A**, left) A Pil1-deficient strain (KKY 0233) expressing Slm1-GFP exhibited an abnormal distribution of Slm1-GFP at 30°C. (**A**, right) Loss of Slm1 (KKY 0236) appears not to cause any defects in the organization of Pil1-GFP-carrying eisosomes at 30°C. (**B**) Localization of Pil1-RFP in slm^{ts} mutants was examined at both the permissive (30°C) and the non-permissive temperatures (38°C). (**B**, first row) Pil1-RFP patches were evenly distributed over the cell cortex in WT cells (KKY 0289) at both temperature conditions. (**B**, second row) Pil1-RFP distribution remained preserved at the membrane in *slm1Δ* cells (KKY 0691). (**B**, third and fourth rows) In two temperature-sensitive mutants (*slm1-2slm2Δ* and *slm1-3slm2Δ*), Pil1-RFP localization was significantly disrupted only at the non-permissive temperature, manifested by few membrane Pil1-RFP patches and a notable increase in cytoplasmic Pil1-RFP fluorescence intensity.

somal compartments or the vacuole (Huckaba *et al.* 2004; Toshima *et al.* 2006). In light of our finding that *slm*^{ts} mutants exhibited noticeable defects in the actin cytoskeleton organization (i.e. disruption in actin patch polarization and aberration in actin cable structure even at the permissive temperature), we set out to test whether the actin defects caused by *SLM* gene mutations are correlated with the extent and severity of the intracellular trafficking of the endosome. The lipophilic dye FM4-64 was used to mark early endosomes as described before (Nannapaneni *et al.* 2010). Briefly, the cells were incubated with 12 μM of FM4-64 for 10 min at the permissive temperature (30°C), washed three times to remove the excess dye and incubated for 3–4 min prior to time-lapse live-cell imaging of the FM4-64-labelled endosome with a frame rate of 4 images per second for 40 s. The rationale for using FM4-64 to mark the endosome in this study was based on the fact that actin patch markers such as Abp1 and Sla1 dissociate from the internalizing patches, making them inadequate for studying the post-internalization endosome motility (Kaksonen *et al.* 2003). In contrast, FM4-64 first labels endocytic patches at the membrane and then the endosomes that fuse later with the vacuole, thus serving as a good marker for the study of cytoplasmic endosomal movement and fusion with vacuoles (Vida and Emr 1995). To assess only the endosome motility, we tracked the movement of 10 mobile endosomes carrying FM4-64 and obtained a representative MSD (mean squared displacement, μm^2) curve for each strain. We found that most of the observed endosome in WT, *slm1Δ* and *slm2Δ* cells moved randomly, although some endosome showed directional movement, as in figure 5A. As expected, the MSD values for those cells increased proportionally over 5 s (figure 5B). The increase in the MSD values for the three *slm*^{ts} mutants over time was less obvious as compared with those of WT and single *slm* mutants (figure 5B), suggesting that the endosome motion in *slm*^{ts} mutants was restrained. Consistently, the representative traces for endosome movement of those mutant cells (figure 5A) showed less endosome motility when compared with WT. It is interesting to note that the endosome motility defects found in *slm1-2* and *slm1-3* cells were no worse than that of *slm1-5*, although the latter exhibited minor actin defect (figure 4B). This indicates that the partial actin disruption caused by *slm1-5* mutation at the permissive temperature (30°C) is sufficient to slow endosome motility. Hence, we conclude that the slow FM4-64 transit to the vacuole (figures 3 and 5) at the permissive temperature is largely due to the slow traffic of FM4-64-carrying endosomes in *slm*^{ts} mutants.

3.6 *Slm proteins are not required for receptor-mediated endocytosis*

Although it has been shown that RME of Fur4 at MCC in *slm*^{ts} cells was impaired at an elevated temperature (40°C), the potential role of Slm proteins on the endocytosis of Abp1-carrying classic RME vesicle has not been reported. Abp1, an actin-binding protein, faithfully reports the RME event of endocytic internalization occurring at the cell surface (Kaksonen *et al.* 2005; Nannapaneni *et al.* 2010). It arrives at the endocytic sites approximately 5–8 s prior to the scission of endocytic vesicles and associates with internalizing endocytic vesicles that undergo longer and faster movement in a directed fashion (Kaksonen *et al.* 2003; Kim *et al.* 2006). To test the effects of the loss of Slm proteins on the internalization of endocytic patches, we examined the behaviour of Abp1-RFP from its appearance at the endocytic sites to its dissociation from the post-internalized endocytic vesicles. We used kymographs to follow the temporal dynamics of individual endocytic sites carrying Abp1-RFP at the cell cortex (figure 6A). From the kymographic analysis, the lifespan of Abp1-RFP in *slm1Δ* and *slm1*-3 appeared to be similar to that of WT. Using a patch track function controlled by SlideBook (v5), we manually determined the membrane lifespan of Abp1-RFP at both the permissive and non-permissive temperatures (figure 6B). At 30°C, the membrane lifespan (9.3±2.5 s) of Abp1-RFP in WT cells was similar to those in the other cells (the mean lifespan is 7.4, 7.8, 11.2, 8.5 and 8.9 s for *slm1Δ*, *slm2Δ*, *slm1-2*, *slm1-3* and *slm1-5* cells, respectively) with *P*-values higher than 0.05 in all five *t*-tests, suggesting the Abp1-RFP lifespan difference between strains are not statistically significant. At the non-permissive temperature, the difference in the membrane lifespan of Abp1-RFP between WT (8.8±2.6 s) and *slm* mutant cells (10.7, 9.6 and 10 s for *slm1Δ, slm1-3,* and *slm1-5*, respectively) was not statistically significant (*P*-values>0.05). However, the lifespans in *slm2Δ* (6.4 s) and *slm1-2* (12.7 s) were statistically different from that of WT (*P*-value<0.03). We next monitored the dynamic behaviour of Abp1-RFP from its appearance to disappearance by creating the path of a representative patch for each strain (figure 6C). The representative track of an individual Abp1-RFP for each strain illustrates directed motion after it moves away from its site of formation. We further investigated the character and degree of Abp1-RFP motility by plotting MSD values over time, with the aid of a particle tracking software as described before (Kim *et al.* 2006). As shown in figure 6D, the initial phase of each MSD curve of Abp1-RFP for first 6–7 s was close to the horizontal straight line of the MSD plot, indicating that patches were stationary. After moving away from their place of origin, Abp1-RFP patches in WT cells showed directed motion, manifested by the slope of MSD curve increasing dramatically (figure 6D). Interestingly, the resulting MSD curves for *slm* mutant cells (*slm1Δ*, *slm1-2* and *slm1-3*) were not significantly different from that for WT cells, suggesting that Slm proteins are not required for actin-based patch motility (figure 6D).

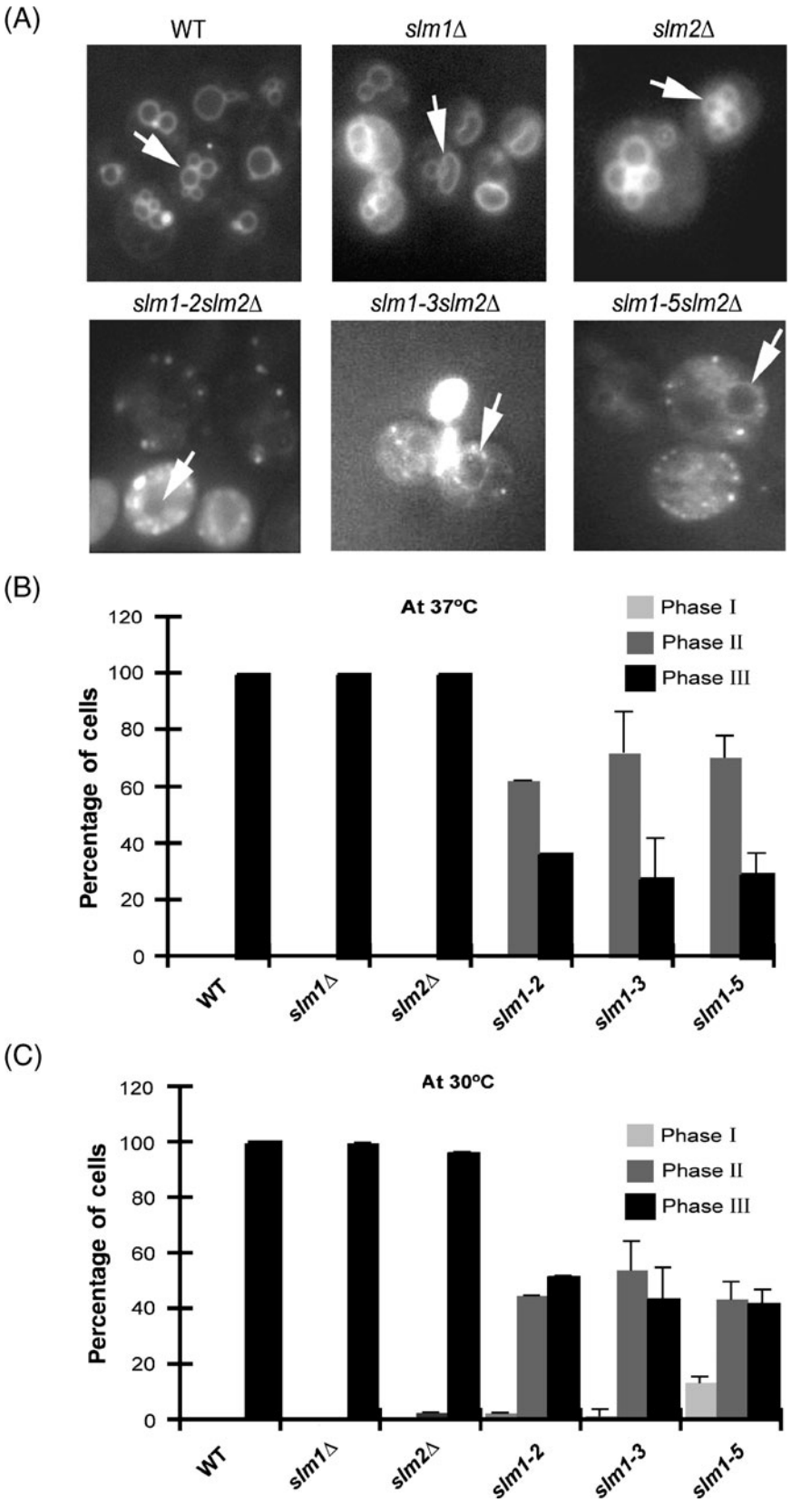

Figure 3. For caption, *see* page no. 89.

3.7 *Impaired membrane recycling in slm1-3 cells*

The accumulation and slow traffic of FM4-64 foci in *slm*^{ts} cells (figures 3 and 5) were reminiscent of those seen in *rcy1Δ* cells in which the recycling of FM4-64 back to the plasma membrane was strongly inhibited (Wiederkehr *et al.* 2000). To test whether the abnormal FM4-64 accumulation in *slm*^{ts} cells was in part due to a defect in recycling, a real-time FM4-64 recycling assay was performed along with a positive control (*rcy1Δ*) at room temperature for 10 min. FM4-64 fluorescence in WT as well as *slm1Δ* cells decreased to ~60% of the initial value by 10 min (figure 7A), consistent with the published result (Wiederkehr *et al.* 2000). Experiments with *slm1-3* showed that recycling of FM4-64 was clearly slower than those of WT and *slm1Δ* cells. In light of the previous observation of no actin defect in *slm*^{ts} cells at room temperature (Fadri *et al.* 2005), we hypothesized that membrane recycling occurs in an actin-independent manner. To test the hypothesis, we first examined whether an intact actin cytoskeleton is present in mutant cells defective in membrane recycling, including *rcy1Δ*, *tlg1Δ* and *tlg2Δ* cells. As shown in figure 7B, no detectable actin defects were found in those cells. Next, we measured the rate of FM4-64 recycling in a formin temperature-sensitive mutant (*bni1-12bnr1Δ*) that loses the actin cable completely at the restrictive temperature (38°C) (Evangelista *et al.* 2002). As expected, the total fluorescence intensity of FM4-64 in the mutant decreased to~60% of the initial value after 10 min, similar to the level for WT cells (figure 7C), suggesting that membrane recycling occurs in an actin-independent manner.

4. Discussion

Among the MCC components, Slm proteins are well known for their essential roles in cell growth and in the organization of the actin cytoskeleton. In this study, we discovered that Slm1 colocalizes with Pil1, a central organizer of eisosome, but minimally with the MCP marker Pma1 and that at least one of the functional Slm homologues is required for the organization of the eisosome. Next, the disorganization of the actin cytoskeleton caused by the inactivation of Slm proteins profoundly affects the motility of post-internalized endosomes *en route* to the vacuole. Finally, we found that membrane recycling is impaired in *slm*^{ts} cells in an actin-independent manner.

4.1 *Potential roles of Slm proteins in eisosome organization*

Our data shows that Pil1 was severely dislocalized from eisosome upon inactivation of Slm1 in a *slm2Δ* background at the non-permissive temperature, suggesting a potential role of Slm proteins in eisosome organization. Considering that two Slm1 mutant proteins in *slm1-2* and *slm1-3* cells were found to be abnormally accumulated in the cytoplasm at the non-permissive temperature (Audhya *et al.* 2004), it is probable that the proper spatial localization of Slm proteins to eisosome is required for exerting their optimal functions in organizing actin structure as well as maintaining structural stability of the eisosome. One important question is how Slm proteins contribute to the eisosome organization. Interestingly, the fewer and weaker Pil1-RFP foci near the cell cortex and the cytoplasmic dispersion of Pil1-RFP (figure 2) are reminiscent of the phenotypes observed in phospho-mimicking *pil1(4D)* mutant cells, which display cytoplasmic Pil1-GFP with only a few punctuate Pil1 dots at the membrane (Walther *et al.* 2007). Therefore, one possible explanation for our observation would be that Pil1 might be hyperphosphorylated and subsequently dissociated from eisosome as Slm1/2 are physically not present at the eisosome. As Pil1 is a direct substrate of Pkh1/2-kinases (Zhang *et al.* 2004; Walther *et al.* 2007; Luo *et al.* 2008), it is not unreasonable to speculate that the phosphorylation activity and/or levels of Pkh1/2 are elevated in cells lacking Slm activity. Furthermore, a previous study revealed that Nce102, an eisosome marker, serves as an upstream negative regulator of Pkh1 (Frohlich *et al.* 2009). It would thus be of great interest to investigate the possibility of down-regulation of Nce102 or hyperactivation of Pkh1/2 in response to inactivation (or dissociation from the eisosome) of Slm proteins.

Figure 3. The *slm*^{ts} mutants displayed defects in FM4-64 transport even at the optimal temperature (30°C). FM4-64 pulse-chase experiments were performed as described in the Methods section. Cells were incubated with FM4-64 for 30 min either at 30°C or 37°C before imaging. (**A**) Representative FM4-64 fluorescence images of WT (KKY 0197), *slm1Δ* (KKY 0193), *slm2Δ* (KKY 0299), *slm1-2slm2Δ* (KKY 0323), *slm1-3slm2Δ* (KKY 0324) and *slm1-5slm2Δ* (KKY 0326). FM4-64 stained primarily the vacuole membrane (ring staining pattern) in WT, *slm1Δ* and *slm2Δ* cells, as indicated by the arrows. The vacuole membrane staining of FM4-64 was less obvious in *slm*^{ts} mutants, but a diffuse cytoplasmic pattern of FM4-64 staining was observed instead. This result indicates incomplete transit of FM4-64 to the vacuole in the mutants. (**B**) Quantification of bulk-phase endocytosis at the non-permissive temperature (37°C). On the basis of the subcellular distribution of FM4-64, cells were grouped into one of the three phases (phase I, II and III), as described in the Methods section. We performed the experiment three times to determine the mean value and standard deviation. (**C**) Quantification of bulk-phase endocytosis at the permissive temperature (30°C). The rate of FM4-64 transit to the vacuole decreased significantly, as the majority of *slm*^{ts} mutants were in phase II (FM4-64 in the cytoplasm).

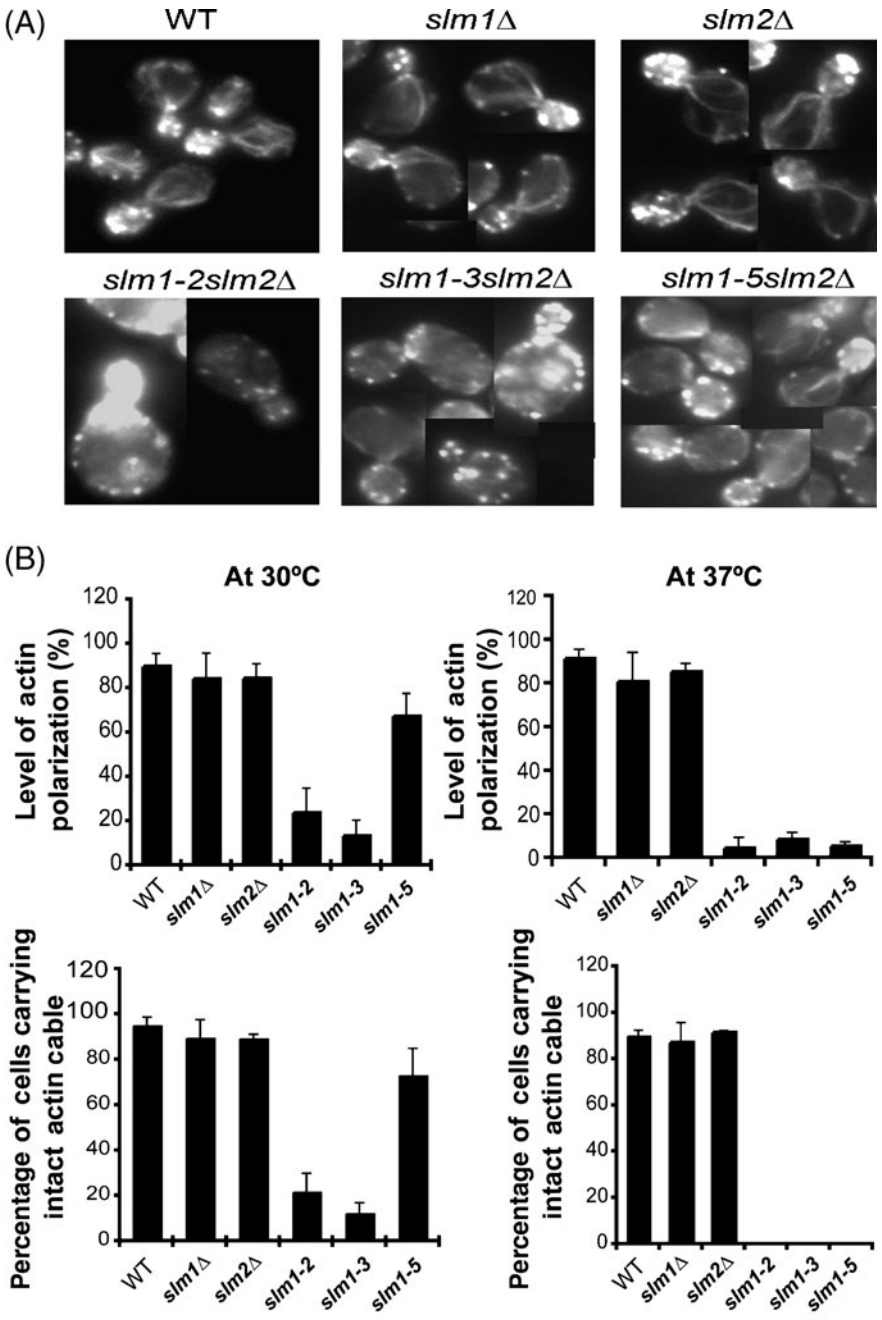

Figure 4. Actin disruption in *slm*^{ts} mutant cells at the optimal (30°C) and the non-permissive (37°C) temperatures. Cells were stained with 3 μM fluorescein isothiocyanate (FITC)-Phalloidin and subjected to a fluorescence microscopic analysis. (**A**) Representative images of the actin cytoskeleton at 30°C. Polarization of actin patches as well as intact longitudinal actin cables were seen in WT, *slm1Δ* and *slm2Δ* cells. Defects in actin polarization and actin cable formation were obvious, particularly in *slm1-2* and *slm1-3* cells. (**B**) Quantifications of the extent of actin patch polarization and actin cable formation at both the permissive (30°C) and non-permissive (37°C) temperatures. Actin is defined as polarized if the mother portion of small-budded cells contains <5 actin patches. A vast majority of *slm1-2* and *slm1-3* cells showed depolarized actin patches. Actin cables were defined as intact if they ran parallel to the longitudinal axis of the cell. Cells displaying fragmented short actin cables or lacking a detectable actin cables were excluded from the intact actin cable group.

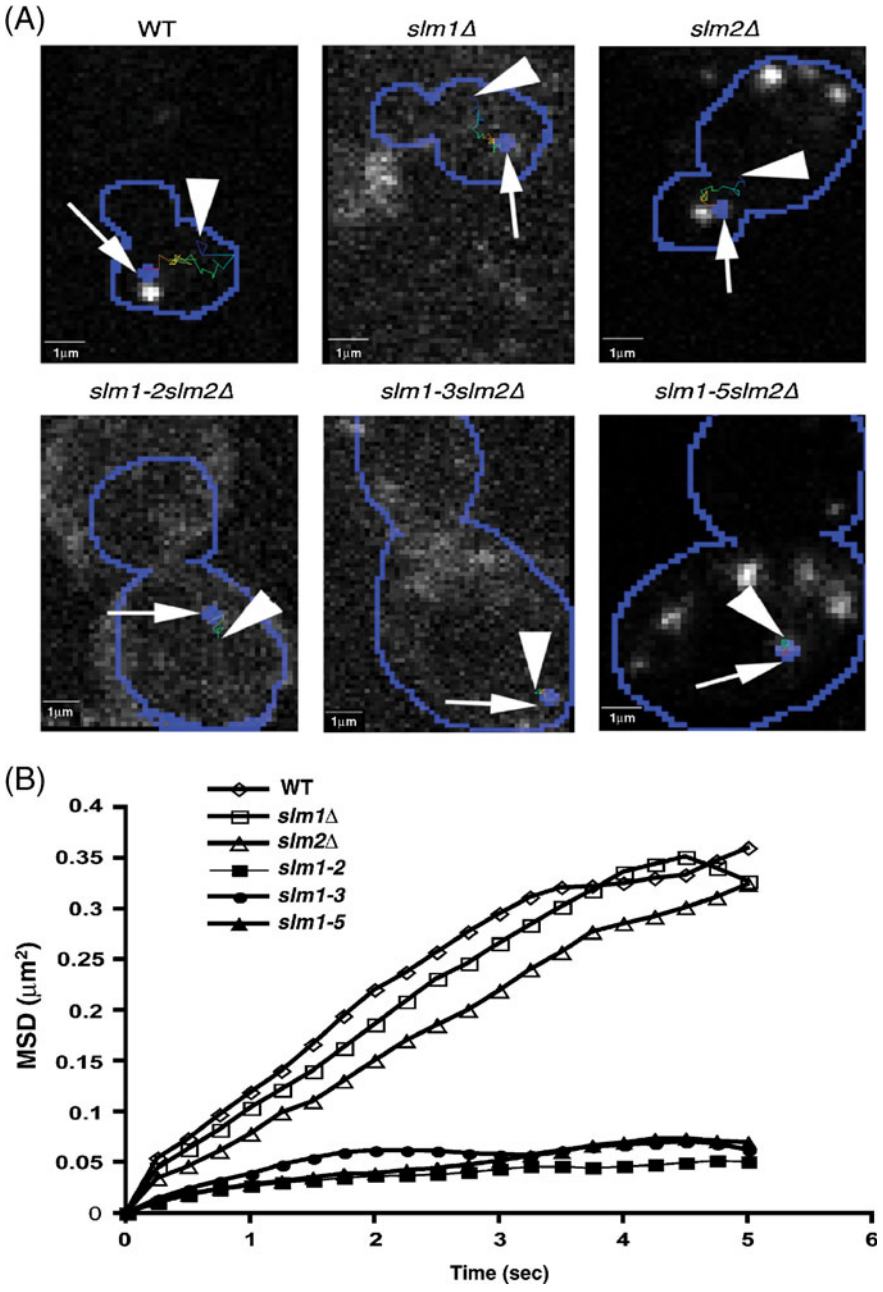

Figure 5. Perturbation of endosome motility in *slm*^{ts} mutant cells. Time-lapse fluorescence images of FM4-64-labelled endosomes were recorded with frame rate of 4 images/s. (**A**) Representative tracks (for 5 s) of endosomes. The trajectories of selected endosomes from WT, *slm1* and *slm2* showed directed motion. The starting and ending positions of each trajectory are indicated by arrowheads and arrows, respectively. In *slm*^{ts} mutants, long-range endosome motions were not observed. (**B**) Quantitative analysis of FM4-64-labelled endosome motility. A total of 10 moving endosomes were tracked from each strain to generate the MSD (mean squared displacement, μm^2) curves. The MSD value for only 5 s are shown here.

4.2 *Slm proteins in endocytic trafficking from the plasma membrane to the vacuole*

A group of researchers (Bultynck *et al.* 2006) clearly demonstrated the significance of Slm proteins in Fur4 endocytosis. They found that the ubiquitinated Fur4 was fairly stable during heat stress and accumulated at the plasma membrane in cells lacking Slm protein activity, and therefore proposed that Slm proteins are required for Fur4 internalization only during heat shock. In the same article, they noted an analysis of Lucifer yellow (LY) that revealed no difference between WT and *slm*^{ts} mutant cells at 37°C, and concluded that Slm proteins were not required generally for endocytosis. Undoubtedly, the membrane-

impermeant fluorescent dye LY is an ideal fluid-phase endocytic marker that is taken up by the endocytic machinery, trapped within the 'fluid-phase' of endocytic vesicles and eventually delivered to the vacuole (Riezman 1985; Dulic *et al.* 1991). However, it is important to note that another lipophilic fluid-phase endocytosis marker, FM4-64, incorporates into endocytic vesicle membranes and becomes highly fluorescent in lipid environments (Betz *et al.* 1996; Fischer-Parton *et al.* 2000), and is thereby better suited for the study of trafficking of endocytic vesicle compartments to the vacuole. Therefore, in this study we took advantage of the FM4-64 pulse-chase assay to assess a possible subtle abnormality in endocytic trafficking and found that FM4-64 was significantly accumulated in the cytoplasm in slm^{ts} cells even at a favourable growth temperature (30°C) (figure 3). Taken together, it is thus possible that such a defect in the FM4-64 transit found in our experiment could have been overlooked in the previous study that used LY. In addition, we found that such an abnormality is attributed to slow FM4-64-carrying endosome motility in the cytoplasm *en route* to the vacuole, perhaps caused by a partially disrupted actin cytoskeleton in those slm^{ts} mutants (figures 4 and 5). Our results are in agreement with the emerging view that an intact F-actin system is required for efficient post-endocytic traffic (Huckaba *et al.* 2004; Toshima *et al.* 2006). The accumulation of FM4-64 in the slm^{ts} mutant(s) indicates that the endosomal trafficking to the vacuole is impaired at the optimal condition, albeit not completely because of the presence of faint vacuolar rim staining of FM4-64 (figure 3). Despite there being severe defects in the actin cytoskeleton at both permissive and non-permissive conditions (figure 4), the slm^{ts} mutants displayed no defects in the actin-based endocytic patch assembly and its following internalization motility (figure 6), providing an argument against the notion that the severity of the endocytic defect is generally correlated with the severity of the actin phenotype.

4.3 *Implication of Slm proteins in membrane recycling*

We have demonstrated that the accumulation of the trapped FM4-64-carrying endocytic compartments in the cytoplasm (figure 3) is in part due to a recycling defect. This is based on the observation in a real-time recycling assay that the cell-associated FM4-64 fluorescence intensity in slm^{ts} mutants even at the optimal temperature (25°C) decreased at a slower rate when compared with those in WT and *slm2Δ* cells (figure 7). As slm^{ts} mutants have no noticeable defects in the actin cytoskeleton organization at the optimal temperature (Fadri *et al.* 2005), it is evident that intact F-actin filaments were not required for proper recycling in the *slm1-3* mutant. Similarly, a conditional formin mutant (*bni1-12bnr1Δ*) lacking actin cables at the restricted temperature (37°C) (Evangelista *et al.* 2002) showed no detectable defects in membrane recycling (figure 7). Therefore, we have come to the conclusion that an intact actin structure is not required for proper recycling. One important question then is how do recycling vesicles move in an actin-independent manner prior to returning to the plasma membrane. It appears that membrane recycling occurs at a faster rate, as nearly half of the externally introduced FM4-64 recycled within 10 min (Wiederkehr *et al.* 2000). Thus, one hypothesis is that recycling vesicles move passively in an actin-independent manner by utilizing the pushing power of the force that pushes the vesicle away from the plasma membrane. Although it remains unelucidated as to whether or not the majority of recycling vesicles are confined to the vicinity of the plasma membrane, it is highly possible that retrieval and recycling of bulk membrane components occur more efficiently if the uptake takes place near the site of their insertion. However, studies have showed that the movement of post-internalized actin patches and endocytic vesicles carrying Ste2 were found to depend on the *de novo* actin assembly (Winter *et al.* 1997; Carlsson *et al.* 2002; Chang *et al.* 2003), although the efforts to visualize F-actin filaments and its associated proteins on those vesicles were unsuccessful. We suspect that the actin polymerization machinery exists on the motile vesicles at a concentration below the detection limit but sufficient to drive those vesicles. Along with this local recycling pathway transporting the trapped materials directly from the early-sorting endosome to the membrane, the remaining endosomes have been known to travel to pass the trans-Golgi network (TGN) before returning to the plasma membrane (Lewis *et al.* 2000; Wiederkehr *et al.* 2000; Ortiz and Novick 2006). In yeast, the requirement for the actin cytoskeleton in vesicle

Figure 6. Inactivation of *SLM* genes is not accompanied by a noticeable defect in receptor-mediated endocytosis. Time-lapse fluorescence images of Abp1-RFP patches were recorded with frame rate of 3 images/s. (**A**) Kymograph representation of Abp1-RFP in a single patch at the cell cortex over time in WT, *slm1* and *slm1-3*. As shown in thekymographs, there was no noticeable difference in the membrane lifespan of Abp1-RFP between cells. (**B**) Assessment of the lifespan of Abp1-RFP patches on the membrane. The graph shows mean and standard deviation values of lifespan of Abp1-RFP patches on the plasma membrane. Membrane lifespans of at least 10 Abp1-RFP patches were manually determined as described in the Methods section. (**C**) Tracks of Abp1-RFP patch movement. A representative Abp1-RFP patch track for each strain is shown, from its appearance on the membrane (arrow) to its disappearance (arrowhead). All representative Abp1-RFP patches here showed directed motion before they disappeared. Each pixel represents 130 nm (7.7 pixels are approximately equal to 1 μm). (**D**) Quantitative Abp1-RFP patch motion analysis. The MSD curve vs. time for each strain was obtained by tracking at least 10 Abp1-RFP patches.

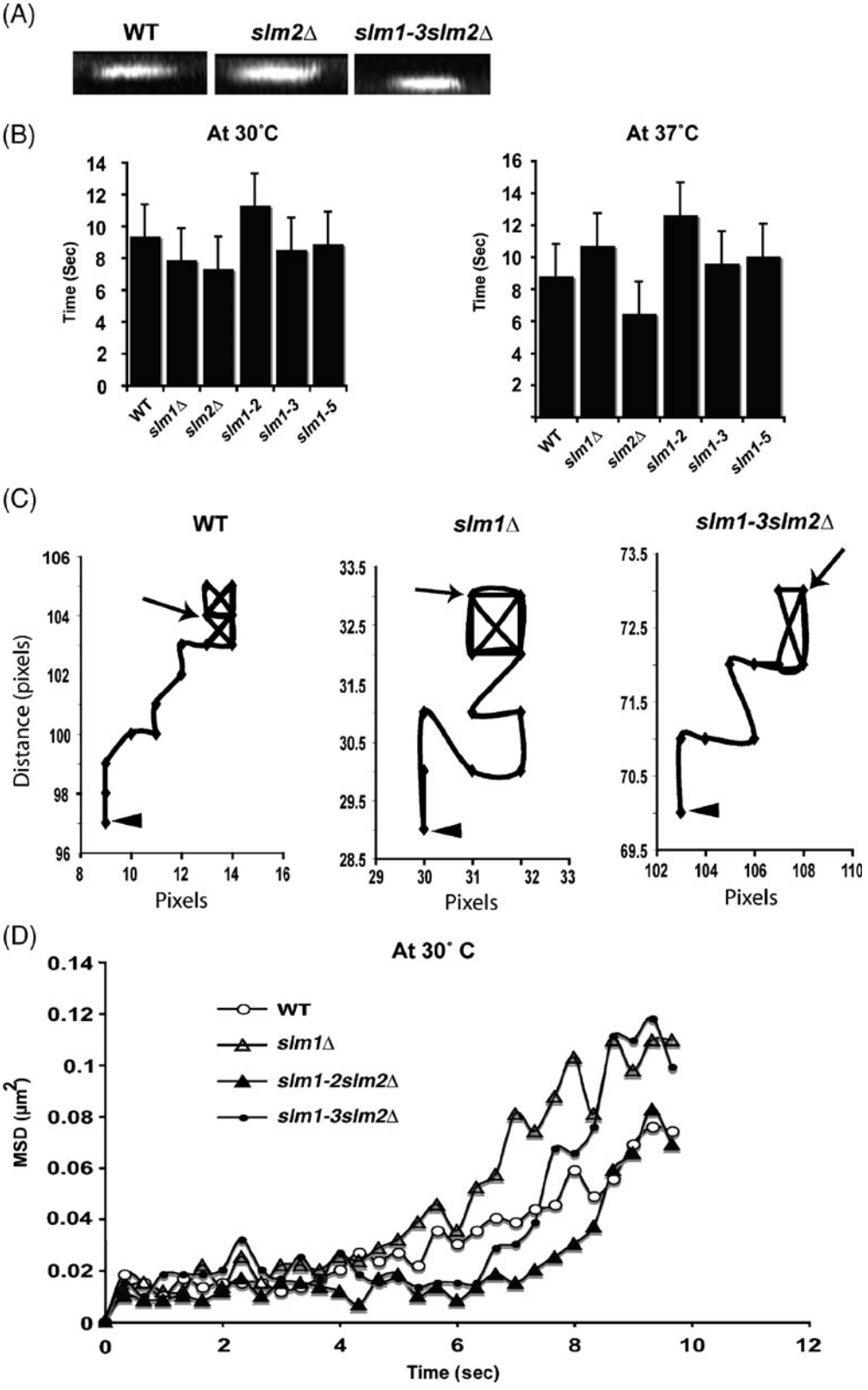

Figure 6. For caption, *see* page no. 92.

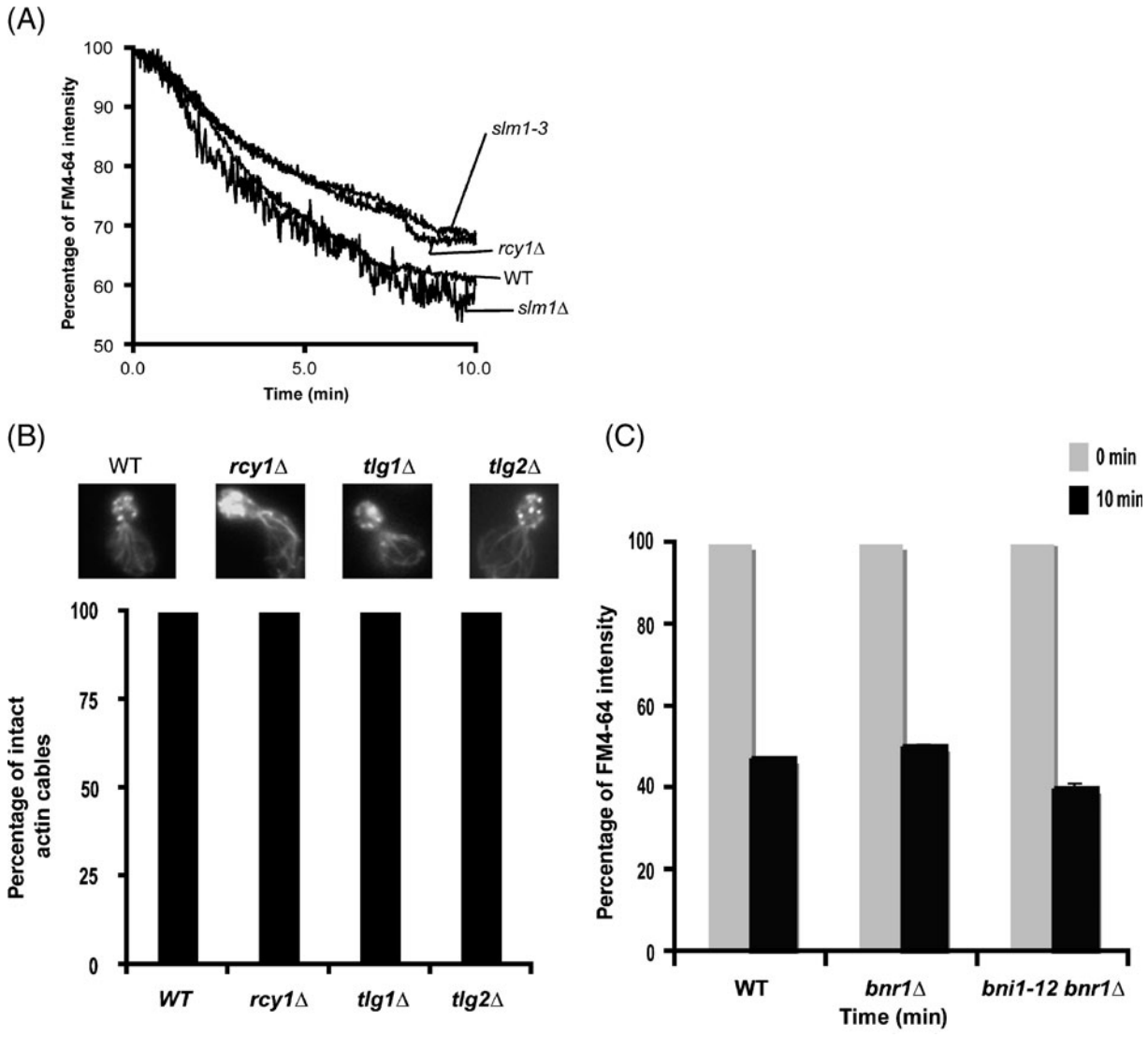

Figure 7. *slm*^{ts} mutant displayed a defect in recycling of FM4-64. (**A**) A real-time FM4-64 recycling assay in WT (KKY 0197), *slm1* (KKY 0193), *slm1-3* (KKY 0324) and *rcy1* (KKY 0082). FM4-64 fluorescence in the cell suspension was measured for 10 min continuously in a spectrofluorometer. (**B**) Actin cable quantification. Cells were stained with 3 μM fluorescein isothiocyanate (FITC)-Phalloidin. Quantifications of the extent of intact actin cable formation were made in WT (KKY 0197), *tlg1* (KKY 0491), *tlg2* (KKY 0492) and *rcy1* (KKY 0082) at the permissive (30°C) temperature. Representative images of the intact actin cable are included. (**C**) FM4-64 recycling assay was performed in WT (KKY 0197), *bnr1* (KKY 0038) and *bni1-12bnr1* (KKY 0040) at 38°C. FM4-64 fluorescence intensities at the starting (0 min) and the ending (10 min) times are shown as bars.

trafficking from the endosomes to the plasma membrane through the TGN remains to be clarified, except for the known fact that the F-actin motor Myo2 is required for the Golgi–plasma membrane traffic (Lipatova *et al.* 2008). Whether the yeast cytoplasmic F-actin bundles (actin cables) are useful tracks of the recycling vesicles heading to the TGN is not known. In higher eukaryotes, it has been proposed that short-range traffic of endocytic compartments is mediated by myosin VI, a plus-ended motor that travels along the actin cytoskeleton (Sweeney and Houdusse 2007). However, the yeast *Saccharomyces cerevisiae* does not express Myosin VI but five other myosins: two type V myosins (Myo2 and Myo4) that direct the motility of secretor vesicles, organelles and mRNAs, a conventional myosin (Myo1) that involves in cytokinesis and two type I myosins (Myo3 and Myo5) (Goode and Rodal 2001; Balasubramanian *et al.* 2004; Pruyne *et al.* 2004). Thus, the concept of acto-myosin cytoskeleton playing a role in recycling vesicle traffic is still alive and needs to be tested to fully appreciate the significance of it.

Acknowledgements

We are grateful to Scott Emr for providing *slm*^{ts} mutant strains and Mark Longtine for providing the PCR templates. We thank Paul Durham and Mark Richter for providing unrestricted access to laboratories and equipment. This work was supported by a National Scientific Foundation Grant 0923024 (to KK) and by thesis funding from Missouri State University (to CK).

References

Abe M, Qadota H, Hirata A and Ohya Y 2003 Lack of GTP-bound Rho1p in secretory vesicles of *Saccharomyces cerevisiae*. *J. Cell Biol.* **162** 85–97

Audhya A and Emr SD 2002 Stt4 PI 4-kinase localizes to the plasma membrane and functions in the Pkc1-mediated MAP kinase cascade. *Dev. Cell* **2** 593–605

Audhya A and Emr SD 2003 Regulation of PI4,5P2 synthesis by nuclear-cytoplasmic shuttling of the Mss4 lipid kinase. *EMBO J.* **22** 4223–4236

Audhya A, Loewith R, Parsons AB, Gao L, Tabuchi, M, Zhou H, Boone C, Hall MN and Emr SD 2004 Genome-wide lethality screen identifies new PI4,5P2 effectors that regulate the actin cytoskeleton. *EMBO J.* **23** 3747–3757

Balasubramanian MK, Bi E and Glotzer M 2004 Comparative analysis of cytokinesis in budding yeast, fission yeast and animal cells. *Curr. Biol.* **14** R806–818

Betz WJ, Mao F and Smith CB 1996 Imaging exocytosis and endocytosis. *Curr. Opin. Neurobiol.* **6** 365–371

Blondel MO, Morvan J, Dupre S, Urban-Grimal D, Haguenauer-Tsapis R and Volland C 2004 Direct sorting of the yeast uracil permease to the endosomal system is controlled by uracil binding and Rsp5p-dependent ubiquitylation. *Mol. Biol. Cell* **15** 883–895

Bultynck G, Heath VL, Majeed AP, Galan JM, Haguenauer-Tsapis R and Cyert MS 2006 Slm1 and slm2 are novel substrates of the calcineurin phosphatase required for heat stress-induced endocytosis of the yeast uracil permease. *Mol. Cell. Biol.* **26** 4729–4745

Carlsson AE, Shah AD, Elking D, Karpova TS and Cooper JA 2002 Quantitative analysis of actin patch movement in yeast. *Biophys. J.* **82** 2333–2343

Chang FS, Stefan CJ and Blumer KJ 2003 A WASp homolog powers actin polymerization-dependent motility of endosomes *in vivo*. *Curr. Biol.* **13** 455–463

Chevallier MR 1982 Cloning and transcriptional control of a eucaryotic permease gene. *Mol. Cell. Biol.* **2** 977–984

Desrivieres S, Cooke FT Parker PJ and Hall MN 1998 MSS4, a phosphatidylinositol-4-phosphate 5-kinase required for organization of the actin cytoskeleton in *Saccharomyces cerevisiae*. *J. Biol. Chem.* **273** 15787–15793

Dickson RC 2008 Thematic review series: sphingolipids. New insights into sphingolipid metabolism and function in budding yeast. *J. Lipid Res.* **49** 909–921

Drubin DG, Kaksonen M, Toret C and Sun Y 2005 Cytoskeletal networks and pathways involved in endocytosis. *Novartis Found. Symp.* **269** 35–42; discussion 43–36, 223–230

Dulic V, Egerton M, Elguindi I, Raths S, Singer B and Riezman H 1991 Yeast endocytosis assays. *Methods Enzymol.* **194** 697–710

Evangelista M, Pruyne D, Amberg DC, Boone C and Bretscher A 2002 Formins direct Arp2/3-independent actin filament assembly to polarize cell growth in yeast. *Nat. Cell Biol.* **4** 260–269

Fadri M, Daquinag A, Wang S, Xue T and Kunz J 2005 The pleckstrin homology domain proteins Slm1 and Slm2 are required for actin cytoskeleton organization in yeast and bind phosphatidylinositol-4,5-bisphosphate and TORC2. *Mol. Biol. Cell* **16** 1883–1900

Fischer-Parton S, Parton RM, Hickey PC, Dijksterhuis J, Atkinson HA and Read ND 2000 Confocal microscopy of FM4-64 as a tool for analysing endocytosis and vesicle trafficking in living fungal hyphae. *J. Microsc.* **198** 246–259

Frohlich F, Moreira K, Aguilar PS, Hubner NC, Mann M, Walter P and Walther TC 2009 A genome-wide screen for genes affecting eisosomes reveals Nce102 function in sphingolipid signaling. *J. Cell Biol.* **185** 1227–1242

Galan JM, Moreau V, Andre B, Volland C and Haguenauer-Tsapis R 1996 Ubiquitination mediated by the Npi1p/Rsp5p ubiquitin-protein ligase is required for endocytosis of the yeast uracil permease. *J. Biol. Chem.* **271** 10946–10952

Goode BL and Rodal AA 2001 Modular complexes that regulate actin assembly in budding yeast. *Curr. Opin. Microbiol.* **4** 703–712

Grossmann G, Malinsky J, Stahlschmidt W, Loibl M, Weig-Meckl I, Frommer WB, Opekarova M and Tanner W 2008 Plasma membrane microdomains regulate turnover of transport proteins in yeast. *J. Cell Biol.* **183** 1075–1088

Grossmann G, Opekarova M, Malinsky J, Weig-Meckl I and Tanner W 2007 Membrane potential governs lateral segregation of plasma membrane proteins and lipids in yeast. *EMBO J.* **26** 1–8

Homma K, Terui S, Minemura M, Qadota H, Anraku Y, Kanaho Y and Ohya Y 1998 Phosphatidylinositol-4-phosphate 5-kinase localized on the plasma membrane is essential for yeast cell morphogenesis. *J. Biol. Chem.* **273** 15779–15786

Huckaba TM, Gay AC, Pantalena LF, Yang HC and Pon LA 2004 Live cell imaging of the assembly, disassembly, and actin cable-dependent movement of endosomes and actin patches in the budding yeast, *Saccharomyces cerevisiae*. *J. Cell Biol.* **167** 519–530

Kaksonen M, Sun Y and Drubin DG 2003 A pathway for association of receptors, adaptors, and actin during endocytic internalization. *Cell* **115** 475–487

Kaksonen M, Toret CP and Drubin DG 2005 A modular design for the clathrin- and actin-mediated endocytosis machinery. *Cell* **123** 305–320

Kim K, Galletta BJ, Schmidt KO, Chang FS, Blumer KJ and Cooper JA 2006 Actin-based motility during endocytosis in budding yeast. *Mol. Biol. Cell* **17** 1354–1363

Kim K, Yamashita A, Wear MA, Maeda Y and Cooper JA 2004 Capping protein binding to actin in yeast: biochemical mechanism and physiological relevance. *J. Cell Biol.* **164** 567–580

Kurtz JE, Exinger F, Erbs P and Jund R 1999 New insights into the pyrimidine salvage pathway of *Saccharomyces cerevisiae*: requirement of six genes for cytidine metabolism. *Curr. Gen.* **36** 130–136

Lewis MJ, Nichols BJ, Prescianotto-Baschong C, Riezman H and Pelham HR 2000 Specific retrieval of the exocytic SNARE Snc1p from early yeast endosomes. *Mol. Biol. Cell* **11** 23–38

Lipatova Z, Tokarev AA, Jin Y, Mulholland J, Weisman LS and Segev N 2008 Direct interaction between a myosin V motor and the Rab GTPases Ypt31/32 is required for polarized secretion. *Mol. Biol. Cell* **19** 4177–4187

Liu J, Sun Y, Drubin DG and Oster GF 2009 The mechanochemistry of endocytosis. *PLoS Biol.* **7** e1000204

Longtine MS, Mckenzie A 3rd, Demarini DJ, Shah NG, Wach A, Brachat A, Philippsen P and Pringle JR 1998 Additional modules for versatile and economical PCR-based gene deletion and modification in *Saccharomyces cerevisiae. Yeast (Chichester, England)* **14** 953–961

Luo G, Gruhler A, Liu Y, Jensen ON and Dickson RC 2008 The sphingolipid long-chain base-Pkh1/2-Ypk1/2 signaling pathway regulates eisosome assembly and turnover. *J. Biol. Chem.* **283** 10433–10444

Malinska K, Malinsky J, Opekarova M and Tanner W 2004 Distribution of Can1p into stable domains reflects lateral protein segregation within the plasma membrane of living *S. cerevisiae* cells. *J. Cell Sci.* **117** 6031–6041

Nannapaneni S, Wang D, Jain S, Schroeder B, Highfill C, Reustle L, Pittsley D, Maysent A, *et al.* 2010 The yeast dynamin-like protein Vps1:vps1 mutations perturb the internalization and the motility of endocytic vesicles and endosomes via disorganization of the actin cytoskeleton. *Eur. J. Cell Biol.* **89** 499–508

Ortiz D and Novick PJ 2006 Ypt32p regulates the translocation of Chs3p from an internal pool to the plasma membrane. *Eur. J. Cell Biol.* **85** 107–116

Pruyne D, Gao L, Bi E and Bretscher A 2004 Stable and dynamic axes of polarity use distinct formin isoforms in budding yeast. *Mol. Biol. Cell* **15** 4971–4989

Riezman H 1985 Endocytosis in yeast: several of the yeast secretory mutants are defective in endocytosis. *Cell* **40** 1001–1009

Schmidt A, Kunz J and Hall MN 1996 TOR2 is required for organization of the actin cytoskeleton in yeast. *Proc. Natl. Acad. Sci. USA* **93** 13780–13785

Shaw JD, Cummings KB, Huyer G, Michaelis S and Wendland B 2001 Yeast as a model system for studying endocytosis. *Exp. Cell Res.* **271** 1–9

Sizonenko GI, Karpova TS, Gattermeir DJ and Cooper JA 1996 Mutational analysis of capping protein function in *Saccharomyces cerevisiae. Mol. Biol. Cell* **7** 1–15

Sweeney HL and Houdusse A 2007 What can myosin VI do in cells? *Curr. Opin. Cell Biol.* **19** 57–66

Toshima JY, Toshima J, Kaksonen M, Martin AC, King DS and Drubin DG 2006 Spatial dynamics of receptor-mediated endocytic trafficking in budding yeast revealed by using fluorescent alpha-factor derivatives. *Proc. Natl. Acad. Sci. USA* **103** 5793–5798

Vida TA and Emr SD 1995 A new vital stain for visualizing vacuolar membrane dynamics and endocytosis in yeast. *J. Cell Biol.* **128** 779–792

Walther TC, Aguilar PS, Frohlich F, Chu F, Moreira K, Burlingame AL and Walter P 2007 Pkh-kinases control eisosome assembly and organization. *EMBO J.* **26** 4946–4955

Walther TC, Brickner JH, Aguilar PS, Bernales S, Pantoja C and Walter P 2006 Eisosomes mark static sites of endocytosis. *Nature (London)* **439** 998–1003

Wedlich-Soldner R, Altschuler S, Wu L and Li R 2003 Spontaneous cell polarization through actomyosin-based delivery of the Cdc42 GTPase. *Sci. NY* **299** 1231–1235

Wiederkehr A, Avaro S, Prescianotto-Baschong C, Haguenauer-Tsapis R and Riezman H 2000 The F-box protein Rcy1p is involved in endocytic membrane traffic and recycling out of an early endosome in *Saccharomyces cerevisiae. J. Cell Biol.* **149** 397–410

Winter D, Podtelejnikov AV, Mann M and Li R 1997 The complex containing actin-related proteins Arp2 and Arp3 is required for the motility and integrity of yeast actin patches. *Curr. Biol.* **7** 519–529

Yu JW, Mendrola JM, Audhya A, Singh S, Keleti D, DeWald DB, Murray D, Emr SD and Lemmon MA 2004 Genome-wide analysis of membrane targeting by *S. cerevisiae* pleckstrin homology domains. *Mol. Cell* **13** 677–688

Zhang X, Lester RL and Dickson RC 2004 Pil1p and Lsp1p negatively regulate the 3-phosphoinositide-dependent protein kinase-like kinase Pkh1p and downstream signaling pathways Pkc1p and Ypk1p. *J. Biol. Chem.* **279** 22030–22038

MS received 06 October 2010; accepted 09 November 2010

*e*Publication: 14 March 2011

Corresponding editor: DURGADAS P KASBEKAR